# Acyl Carrier Protein 3 Is Involved in Oxidative Stress Response in *Pseudomonas aeruginosa*

Wei Chen[1,2], Bo Wang[3], Jordon D. Gruber[2], Yong-Mei Zhang[2*†] and Christopher Davies[2*]

[1] *Clinical Research Center, The Second Affiliated Hospital of the Southeast University, Nanjing, China,* [2] *Department of Biochemistry and Molecular Biology, Medical University of South Carolina, Charleston, SC, United States,* [3] *Institute of Medicinal Biotechnology, Chinese Academy of Medical Sciences and Peking Union Medical College, Beijing, China*

The human opportunistic pathogen *Pseudomonas aeruginosa* expresses three acyl carrier proteins (ACPs): AcpP, Acp1, and Acp3. The function of AcpP in membrane fatty acid synthesis (FAS) was confirmed recently, but the physiological roles of Acp1 and Acp3 remain unclear. To address this, we investigated the physiological role of Acp3 in *P. aeruginosa*. We found that expression of Acp3 dramatically increases in the log phase of cell growth and that its transcription is under the control of the QS regulators LasR and RhlR. Deletion of *acp3* from *P. aeruginosa strain* PAO1 results in thicker biofilm formation, increased resistance of the strain to hydrogen peroxide, and higher persistence in a mouse infection model. Tandem affinity purification (TAP) experiments revealed several novel protein-binding partners of Acp3, including KatA, the major catalase in *P. aeruginosa*. Acp3 was found to repress the catalase activity of KatA and, consistent with inhibition by Acp3, less reactive oxygen species are present in the *acp3* deletion strain. Overall, our study reveals that Acp3 has a distinct function from that of the canonical AcpP and may be involved in the oxidative stress response.

Keywords: acyl carrier protein, *P. aeruginosa*, virulence, catalase, oxidative stress

## INTRODUCTION

Acyl carrier proteins (ACPs) function in the synthesis of fatty acids, polyketides, and non-ribosomal peptides. In addition to the housekeeping ACP used for Type II fatty acid synthesis (FAS), some bacteria contain specialized variants of ACPs (Geiger et al., 1991; Brozek et al., 1996; Epple et al., 1998; Geiger and Lopez-Lara, 2002; Haag et al., 2009; Ramos-Vega et al., 2009; Chan and Vogel, 2010). Some of these divert intermediates of Type II FAS (FAS) to synthesize molecules like lipid A or hemolysin, whereas others are involved in distinct processes such as polyketide synthesis (Byers and Gong, 2007; Chan and Vogel, 2010). *Rhizobia*, for example, expresses four ACPs (AcpP, NodF, AcpXL, and RkpF), where AcpP is the canonical ACP for FAS and the other three are used for synthesis of cell-surface molecules that facilitate the establishment of symbiosis with their legume hosts (Geiger and Lopez-Lara, 2002). In addition, it was reported recently that in *Salmonella enterica*, an ACP homologue called IacP acylates a type 3 secretion system (T3SS) translocon protein, SipB, leading to insertion of SipB into host-cell membranes (Viala et al., 2017).

By contrast, *Escherichia coli* encodes only a single and essential ACP (De Lay and Cronan, 2007). In addition to functioning in Type II FAS, however, it also acts in several other systems. For instance, the protein interacts with SpoT to switch the activity of SpoT from (p)ppGpp

degradation to (p)ppGpp synthesis during conditions of fatty acid starvation (Battesti and Bouveret, 2006; Angelini et al., 2012) and also forms a complex with the STAS domain of a SLC26 family anion transporter YchM, linking bicarbonate transport with fatty acid metabolism (Babu et al., 2010). In addition, *E. coli* ACP plays an essential role in the biosynthesis of membrane-derived oligosaccharides (MDOs), which are important for osmotic regulation (Therisod et al., 1986). Interestingly, the 4-phosphopantetheine moiety of ACP is not required in the MDO transglucosylation function, a clear difference from ACP's role in fatty acid biosynthesis (Therisod and Kennedy, 1987).

*Pseudomonas aeruginosa* is an opportunistic pathogen that causes life-threatening nosocomial infections and is of particular concern for immunocompromised and cystic fibrosis (CF) patients (Govan and Deretic, 1996). The *P. aeruginosa* genome contains three putative *acp* genes, annotated as PA2966 (*acpP*), PA1869 (*acp1*), and PA3334 (*acp3*). Each contains a conserved serine that is presumed to be the site of 4-phosphopantetheinylation (Raychaudhuri et al., 2005). Recently, AcpP was confirmed as the essential ACP used for membrane FAS, and deletion of *acp1* and *acp3* had minimal effect on cell growth and *in vitro* virulence production (Ma et al., 2017). Previous studies have showed that *acp1* and *acp3* expression is regulated by quorum sensing (QS) (Hentzer et al., 2003; Schuster et al., 2003; Wagner et al., 2003; Chugani et al., 2012) and *acp3* is highly induced during infection (Turner et al., 2014). In particular, the 18-fold increase in expression of *acp3* in an acute infection model and 30-fold increase in a chronic infection model strongly suggests a key role for Acp3 in pathogenicity (Turner et al., 2014). Beyond these indicators, however, the physiological functions of Acp1 and Acp3 in *P. aeruginosa* remain unclear.

In this work, we examined the specific physiological role of Acp3 in *P. aeruginosa via* a combination of transcriptional profiling, western blotting, measuring *in vitro* and *in vivo* virulence, and identification of protein-binding partners. We found that *acp3* is regulated by the QS system and that expression of Acp3 peaks during the early stationary phase of cell growth. Deletion of *acp3* increases biofilm formation, increased resistance of the strain to $H_2O_2$ and higher persistence in the mouse lung. We also found that Acp3 binds and represses the activity of the catalase, KatA. Overall, the data suggest a specialized function for Acp3 involving oxidative response mediated by KatA.

## MATERIALS AND METHODS

### Bacterial Strains, Plasmids, Primers, and Growth Conditions

Bacterial strains and plasmids used in this study are listed in **Table 1**. Strain stocks were maintained at −80°C in 10% glycerol. Bacteria were streaked on fresh plates before each experiment. *P. aeruginosa* and *E. coli* strains were cultured at 37°C in Miller's Luria broth (LB) medium (Sigma-Aldrich) unless specified otherwise. *Pseudomonas* Isolation Agar (PIA) was used for selection of *P. aeruginosa*. Plasmids used for gene knockout were constructed using the described method

(Choi and Schweizer, 2005). Primers used in this study are listed in **Supplementary Table S1**.

To generate expression constructs of *acp1*, *acp3*, *acpP*, *E. coli acp*, and *katA*, the respective genes were amplified and cloned into pEX-HTB vector with restriction and ligation. pEX-HTB is derived from pEX1.8, and encodes a 6x-His tag within its multiple cloning site. All plasmids were confirmed by sequencing. For plasmid maintenance in *E. coli* cultures, the growth medium was supplemented with 50 µg/ml carbenicillin, 30 µg/ml kanamycin, or 30 µg/ml gentamycin. For *P. aeruginosa* cultures, 200 µg/ml carbenicillin or 30 µg/ml gentamycin were used, unless otherwise stated.

### Generation of *acp* Mutant Strains

Unmarked deletion mutants of *P. aeruginosa* were generated using a published method (Choi and Schweizer, 2005). Briefly, the target gene was replaced by a gentamycin ($Gm^r$) resistance cassette through homologous recombination, followed by removal of the cassette by expression of Flp recombinase from pFLP2 and counter selection with 10% sucrose. All mutants were confirmed by PCR using appropriate flanking primers (**Supplementary Table S1**) and DNA sequencing. The deleted DNA fragments corresponded to amino acids 5–79 for Acp1 (94% of the protein sequence) and 7–45 for Acp3 (48% of the protein sequence). For *katA*, the deleted DNA corresponded to amino acids 21–448 (88% of the protein sequence).

### Quantitative RT-PCR of *acp* Transcripts

Transcript levels of *acp* genes were measured by real-time PCR using oligonucleotide primers designed with DNAMAN 7.0 software (Lynnon Cooperation). All primer pairs generated one specific product. The expression of gene *rpoD* was used as the housekeeping control. Cells were harvested at $OD_{600}$ 0.5, 2.0, and 2.6, corresponding to the log, early stationary, and stationary phases, respectively. Total RNA was isolated using RNAqueous kit (Ambion), and genomic DNA was removed by precipitation with LiCl, followed by DNase treatment. cDNA was generated using the High Capability RNA-to-cDNA kit (Ambion), with 1 µg total RNA per reaction. Real-time quantitative PCR was performed in a 96-well plate, using the SensiFAST SYBR® & Fluorescein kit (Bioline). The reaction mixture contained 500 nM gene-specific primers. Amplification and detection were performed on a Bio-Rad MyiQ single-color real time detection system. Experiments were performed in triplicate for each cDNA preparation. No-reverse transcriptase and no-template controls were included for each assay. Data were analyzed by MyiQ software, and the critical threshold cycle ($C_T$) was set automatically. The amounts of *acp* gene mRNA were normalized against *rpoD* gene using the $\Delta\Delta C_T$ method (Rao et al., 2013).

### Protein Expression Profiling

The expression patterns of ACP proteins in *P. aeruginosa* were measured by western blotting. Overnight cultures were used to inoculate 100 ml fresh LB broth with an initial $OD_{600}$ of 0.05, and incubated at 37°C with shaking. Samples were taken every 2 h, and cells lysed in B-PER reagent (Fisher). The total

**TABLE 1 |** Strains and plasmids used in this study.

| Strain or plasmid | Relevant genotype or phenotype | Reference |
|---|---|---|
| ***E. coli* strains** | | |
| JM109 | F′ (traD36, proAB + lacI$^q$ lacZ ΔM15 endA1 recA1 hsdR17($r_k^-$, $m_k^+$) mcrA supE44 λ$^-$ gyrA96 relA1 Δ(lacproAB) | Promega |
| CY1861 | ΔacpP, fabF::Cml, pCY765 | Volkmann et al., 2010 |
| SM10 lpir | thi-1 thr leu tonA lacY supE recA::RP4-2-Tc::Mu Km$^r$ lpir | de Lorenzo and Timmis, 1994 |
| XL-1 blue | recA1, endA1, gyrA96, thl-1, hsdR17, supE44, relA1, lac[F′ proAB lacIq lacZ ΔM15] Tn10 (Tcr) | Parsek et al., 1997 |
| MG4 | Δ(argF-lac)U169, zah-735::T10, recA56, srl::Tn10 | Parsek et al., 1997 |
| ***P. aeruginosa* strains** | | |
| PAO1 | Wild type | Holloway et al., 1979 |
| CW3 | Δacp1, derived from strain PAO1 | This study |
| CW4 | Δacp3, derived from strain PAO1 | This study |
| CW7 | Δacp1Δacp3, derived from strain PAO1 | This study |
| CW14 | ΔpqsR, derived from strain PAO1 | Gruber et al., 2016 |
| CW16 | ΔlasR, derived from strain PAO1 | Gruber et al., 2016 |
| CW17 | ΔrhlR, derived from strain PAO1 | Gruber et al., 2016 |
| CW20 | PAO1 with acpP-SPA in the chromosome | This study |
| CW21 | PAO1 with acp3-SPA in the chromosome | This study |
| CW22 | PAO1 with acp1-SPA in the chromosome | This study |
| CW26 | ΔkatA, derived from strain Δacp3 | This study |
| CW27 | ΔkatA, derived from strain Δacp1Δacp3 | This study |
| CW28 | ΔkatA, derived from strain PAO1 | This study |
| **Plasmids** | | |
| pEX18ApGW | Suicide vector for Pa | Choi and Schweizer, 2005 |
| pEX18ApGW-acp1 | acp1 deletion suicide vector | This study |
| pEX18ApGW-acp3 | acp3 deletion suicide vector | This study |
| pEX18ApGW-pqsR | pqsR deletion suicide vector | This study |
| pEX18ApGW-lasR | lasR deletion suicide vector | This study |
| pEX18ApGW-rhlR | rhlR deletion suicide vector | This study |
| pEX18ApGW-katA | katA deletion suicide vector | This study |
| pEX-HTB | tacp-6His on pEX1.8 | This study |
| pEX-HTB-Acp1 | Acp1 expression vector derived from pEX-HTB | This study |
| pEX-HTB-Acp3 | Acp3 expression vector derived from pEX-HTB | This study |
| pEX-HTB-AcpP | AcpP expression vector derived from pEX-HTB | This study |
| pEX-HTB-KatA | KatA expression vector derived from pEX-HTB | This study |
| pECP61.5 | rhlA′-lacZ transcriptional fusion; tacp-rhlR | de Lorenzo and Timmis, 1994 |
| pKDT17 | lasB′-lacZ transcriptional fusion; tacp-lasR | de Lorenzo and Timmis, 1994 |

protein concentration was determined by Bradford assay. Fifty micrograms of total protein of the whole cell lysates was then separated by SDS-PAGE on 4–20% precast polyacrylamide gels and transferred to a PVDF membrane. SPA-tagged ACP proteins were detected by monoclonal anti-flag M2 (1:5000) (Sigma) and goat anti-mouse IgG-HRP (1:10,000) (Santa Cruz). Images were quantified by the software ImageJ (Schneider et al., 2012).

## Assays for Virulence Phenotypes

For static biofilm formation, cultures of early log phase were diluted into fresh LB to OD$_{600}$ 0.05 and dispensed to a 96-well plate with 100 μl per well. The plate was covered with a transferable solid-phase (TSP) pegged-lid (Nunc) and incubated at 37°C for 18 h without shaking. Biofilms that formed on the pegged lid were washed twice by submerging the lid into a basin of sterilized water and then stained with 0.1% crystal violet (CV)

in a new 96-well plate for 15 min with gentle shaking. Excess CV was washed off with water and then bound CV was eluted from the biofilms into 150 μl of 95% ethanol and quantitated spectrophotometrically at 600 nm using a Biotek Synergy HT plate reader.

## Tandem Affinity Purification

To construct strains expressing sequential peptide affinity (SPA)-tagged ACPs, a 250-bp DNA fragment encoding a calmodulin-binding peptide and 3× FLAG tag separated by a TEV cleavage site (Babu et al., 2009) was synthesized (Genewiz *Inc.*) and fused with a Gm$^r$ cassette by overlapping PCR, generating a SPA-Gm$^r$ fragment. Gene-specific upstream and downstream fragments were fused with this SPA-Gm$^r$ fragment by overlapping PCR and cloned into pEX18ApGw to generate pEX18ApGw-acp1/3/P-SPA. Strains with C-terminal SPA-tagged *acp* were screened and

confirmed by PCR and sequencing (Choi and Schweizer, 2005). SPA-tagged ACP proteins were detected by monoclonal anti-Flag M2 (1:5000) (Sigma) and goat anti-mouse IgG-HRP (1:10,000) (Santa Cruz).

Sequential peptide affinity purification was performed as described previously (Babu et al., 2009). Briefly, SPA-tagged strains and wild-type strain PAO1 were grown in 1 l of Terrific Broth in a 2-l flask at 37°C for 12 h with vigorous shaking. Cell pellets from stationary-phase cultures were harvested and lysed by sonication on ice. The cell lysates were treated with universal nuclease (Pierce) to remove nucleic acids and supplemented with protease inhibitor cocktail (Roche) to protect proteins from hydrolysis. The supernatant was mixed with magnetic beads conjugated with anti-Flag M2 antibody (Sigma) and incubated overnight on a rotary mixer at 4°C. Triton X-100 (0.1%) was added to prevent non-specific binding. The magnetic beads were collected by placing the tube in a magnetic rack, washed until the $OD_{280}$ of flow-through was lower than 0.05, and re-suspended in 200 μl TEV cleavage buffer. TEV protease (40 μl of 1.8 mg/ml) was added and incubated overnight at 4°C with mixing. After the TEV cleavage step was complete, the magnetic beads were collected and the supernatant was transferred to a new tube, to which 400 μl of calmodulin-binding buffer and 1.6 μl of 1 M $CaCl_2$ were added. The solution was then added to calmodulin Sepharose beads (GE Healthcare) and incubated for 3 h at 4°C with gentle mixing. The beads were washed four times with 1 ml of calmodulin-wash buffer (with EGTA). The bound proteins were eluted in 300-μl elution buffer. The target proteins were analyzed by MALDI-TOF mass spectrometry. The entire experiment was repeated once and only proteins identified in both experiments are reported.

## Reverse Pull-Down Assay

A His-KatA expression plasmid, pEXHTB-*katA*, and pEXHTB empty vector control were each transformed into strain CW21 (PAO1 with Acp3-FLAG). Cell pellets were harvested from 1 l of Terrific Broth after 12-h growth and cell lysates were prepared as described above. His-tagged proteins were purified by affinity chromatography using $Ni^{2+}$-NTA agarose (Fisher). Flag-tagged-Acp3 in the elution was detected by western blotting with anti-Flag M2 antibody. Anti-ScKatA antibody was used to detect *P. aeruginosa* KatA (Shin et al., 2008).

## Determination of $H_2O_2$ Sensitivity

The sensitivity of different strains against hydrogen peroxide was determined by the microbroth dilution method in LB. One hundred microliters of a twofold serially diluted $H_2O_2$ solution was aliquoted to a 96-well plate. Cultures of early log phase were diluted in fresh LB to $OD_{600}$ of 0.01 and mixed with $H_2O_2$ solution in equal volume. After incubation for 10 h at 37°C, cell density was measured at $OD_{600}$. To further address the relationship between ACP and $H_2O_2$ resistance, pEX-HTB-derived ACP-expressing plasmids were introduced back into the $\Delta acp1/\Delta acp3$ double mutant. Cultures were incubated in LB supplemented with 2 mM $H_2O_2$

at 37°C with vigorous shaking, and $OD_{600}$ was measured after 5 h.

## Catalase Activity Assay

Catalase activity was measured as described previously (Ou and Wolff, 1996). A standard curve was established by mixing serially diluted $H_2O_2$ with FOX 1 reagent (250 μM ammonium ferrous sulfate, 100 μM xylenol orange, 0.1 M sorbitol, and 25 mM $H_2SO_4$). Cell pellets from 24-h cultures were washed once by PBS and lysed in B-PER reagent (Fisher). After centrifugation, the total protein in the supernatant was determined by Bradford assay. Ten microliters of supernatant was mixed with 990 μl of 200 μM $H_2O_2$ in 50 mM potassium phosphate (pH 7.0) and incubated for 1–30 min at room temperature. Fifty microliters of the mixture was then reacted with 950 μl of FOX 1 reagent at room temperature for 30 min. The reaction mixture was centrifuged and the absorbance of the resultant supernatant was measured at 560 nm. The concentration of remaining $H_2O_2$ was calculated based on the standard curve. The catalase unit activity was defined as the decomposition of 1 μmol of $H_2O_2$ in 1 min by 1 mg of total protein. Three independent experiments were performed. For comparison between replicates, relative catalase activity was calculated.

## Measurement of Intracellular ROS Level

Cell pellets from 10 ml of overnight cultures of wild-type strain and *acp* mutants were harvested, washed, and suspended in 1 ml of PBS. Cell suspensions were treated with 20 μM of 2′,7′-dichlorofluorescein diacetate (DCFH$_2$, dissolved in DMSO) at 37°C for 20 min in the dark. Cells treated with an equal volume of DMSO were used as a negative control. The treated cells were washed once and suspended in 1 ml PBS. Two hundred microliters of suspension was transferred to a black opaque 96-well plate and fluorescence was measured using a BioTek microplate reader at 535 nm emission with excitation at 485 nm. The fluorescence data were normalized to the cell density of each sample. Three independent experiments were performed, and relative fluorescence was calculated by normalization to the wild-type strain for each experiment.

## Mouse Lung Infection Assay

Cells from overnight cultures of the *P. aeruginosa* wild-type strain PAO1 or isogenic *acp* mutant stains were harvested by centrifugation, washed twice and suspended in sterile PBS to $1 \times 10^8$ CFU per 40 μl. Female C57Bl/6J mice (6–8 weeks old, Jackson Laboratories) were inoculated with 40-μl culture *via* oropharyngeal aspiration under anesthesia with isofluorane. Each treatment group contained 10 mice. At 48 h post infection, lungs were harvested, weighed, and homogenized in 1 ml of sterile PBS for bacterial enumeration. *P. aeruginosa* were grown and counted on PIA. The data were analyzed using a Kruskal–Wallis test with *post hoc* Dunn's multiple-comparison tests to compare the bacterial loads among different groups. All procedures were in accordance with a protocol approved by the MUSC Institutional Animal Care and Use Committee.

# RESULTS

## Expression of Acp3 Peaks in the Early Stationary Phase

As a preliminary step to investigate the function of Acp3, we used qRT-PCR to quantify the levels of all three *acp* transcripts in log phase (OD$_{600}$ 0.5), early stationary phase (OD$_{600}$ 2.0), and stationary phase (OD$_{600}$ 2.6). The basal levels of the three transcripts were very different in log phase, with *acp3* being the least abundant and *acpP* the most abundant (**Figure 1A**). Transcript levels of *acp1* and *acp3* increased 9.6-fold and 106-fold, respectively, from log phase to early stationary phase. The level of *acp3* transcript then decreased in stationary phase, whereas that of *acp1* transcript level remained high. By contrast, the level of *acpP* expression remained high throughout, consistent with the expression profile of other known housekeeping *acpP* genes (Zhang et al., 2002).

To determine the endogenous protein levels of the three ACPs, we constructed strains of PAO1 in which the proteins were expressed as fusions with a SPA tag at the C terminus. The SPA tag contains a calmodulin-binding peptide and three FLAG domains. Semi-quantitative western blotting with an anti-Flag M2 antibody was used to measure protein levels at different growth stages. Commensurate with its function in membrane FAS, AcpP was constitutively expressed and also exhibited the highest expression level of the three ACPs (**Figure 1B**). The protein level of Acp3 mirrored its transcriptional pattern, indicating that acp3 expression is mainly regulated transcriptionally. The protein level of Acp1 was the lowest of the three ACPs in log phase, but increased as growth progressed to the stationary phase, which suggests it plays a role during late-stage growth.

## Transcription of *acp3* Is Regulated by QS Regulators

Previous microarray data have indicated that expression of *acp1* and *acp3*, but not *acpP*, are under the control of QS signals in *P. aeruginosa* (Hentzer et al., 2003; Schuster et al., 2003; Wagner et al., 2003). By contrast, a separate study using RNA-seq did not show activation of *acp3* expression by QS (Chugani et al., 2012). To determine whether the transcription of *acp1* and *acp3* is regulated by QS, we measured their respective transcript levels in the QS deletion mutants Δ*lasR*, Δ*rhlR*, and Δ*pqsR* (Gruber et al., 2016). Significantly reduced levels were observed for both *acp1* and *acp3* in the Δ*lasR* and Δ*rhlR* mutants, with at least a 10-fold decrease at an OD of 2.0 for both, but were unchanged in the Δ*pqsR* mutant (**Figure 1C**). Thus, it appears that expression of *acp1* and *acp3* are regulated by both LasR and RhlR systems, but not PqsR. By contrast, the level of the *acpP* transcript was unaffected in all QS mutants.

## Deletion of *acp3* Increases Bacterial Persistence of *P. aeruginosa* in the Murine Model

Next, we investigated whether deletion of *acp3* had any effect on biofilm formation or *in vivo* pathogenicity. Compared to wild
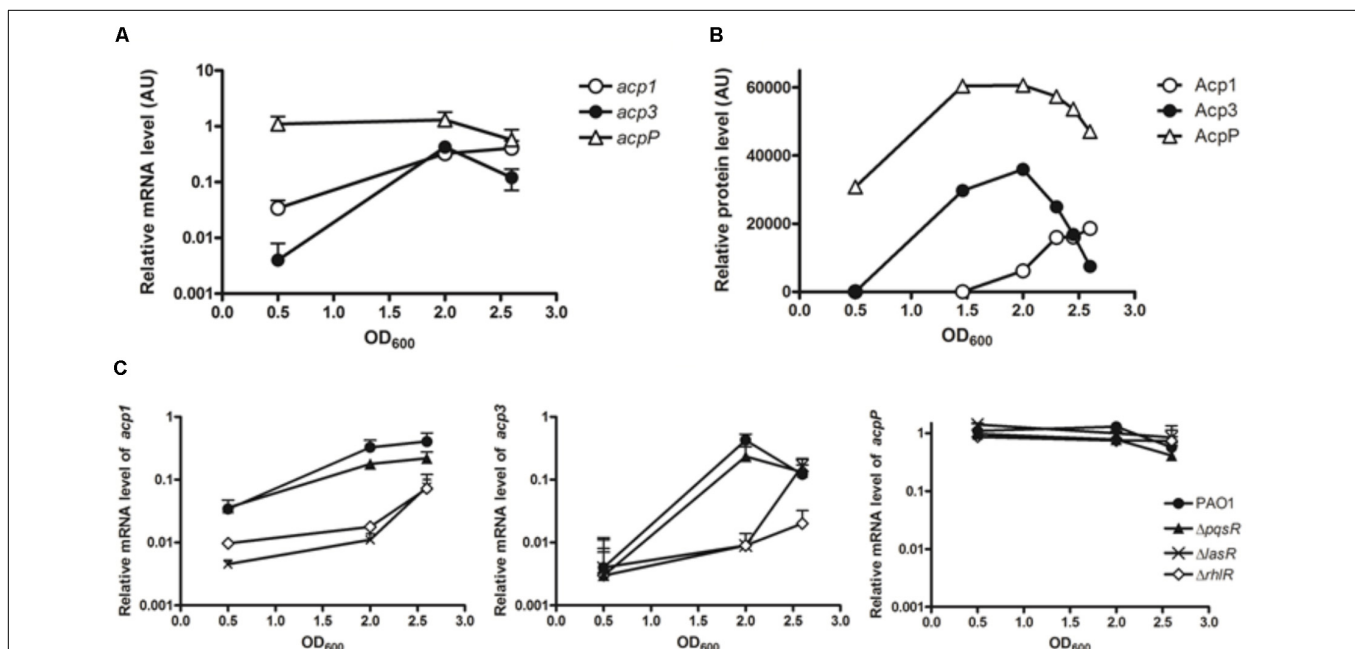


**FIGURE 1 |** Expression profiles of the three *acp* genes in PAO1. **(A)** Transcripts levels were measured by qRT-PCR in log phase (OD$_{600}$ 0.5), early stationary phase (OD$_{600}$ 2.0), and stationary phase (OD$_{600}$ 2.6). **(B)** Expression patterns of three ACP proteins in PAO1 were determined by western blotting with anti-Flag antibody. Samples were taken every 2 h post of inoculation. The immunoblot image was quantified with software ImageJ. **(C)** Regulatory connection between Acp1 and Acp3 and quorum sensing. Levels of *acp1* and *acp3* transcripts are lowered in the QS-deficient mutants, Δ*lasR* and Δ*rhlR*, but not Δ*pqsR*. *acp1*, left panel; *acp3*, middle panel; *acpP*, right panel.

**FIGURE 2 |** Deletion of *acp3* increases biofilm formation and persistence of *P. aeruginosa* PAO1 in a mouse lung infection model. **(A)** Biofilm formation increased in *acp* mutants. Biofilm formation by PAO1 and *acp* mutants was determined using a pegged lid 96-well plate. Data are presented as means ± SEs from three independent experiments. Student's *t*-test was performed between PAO1 and *acp* mutant. * indicates $p < 0.01$. **(B)** Determination of pathogenicity of *acp* mutants *in vivo*. Overnight cultures of wild-type and *acp* mutants were used to infect mice lungs. Forty-eight hours post inoculation, mice were sacrificed, lungs were removed and homogenized, and bacteria were counted on a PIA plate. Two independent experiments were performed. Data are presented as log (CFU/ml) analyzed using a Kruskal–Wallis test with *post hoc* Dunn's multiple-comparison tests among different strains. Short bars within the data indicate the median CFU/ml. Significant *p* values are indicated by [#]$p < 0.05$ and [*]$p < 0.01$.

type, strains with single deletions of *acp1* or *acp3* enhanced static biofilm formation, but the effect was more pronounced in the double mutant (**Figure 2A**). This suggests that Acp1 and Acp3 each contribute to the virulence of *P. aeruginosa*. Additionally, all *acp* deletion strains exhibited higher bacterial loads in the lungs of C57Bl/6J mice, suggesting higher persistence *in vivo*, although the difference between the *acp1* mutant and PAO1 was not significant (**Figure 2B**). The strongest effect was observed with the *acp1/acp3* double mutant, for which the average colony-forming units (CFU) increased approximately three log units. Overall, these data suggest that deletion of *acp3* increases the pathogenicity of *P. aeruginosa*.

## Protein-Binding Partners of *P. aeruginosa* ACPs

To probe the physiological role of Acp3 further, we used tandem affinity purification (TAP) to identify its protein-binding partners, and alongside, the same for Acp1 and AcpP. Proteins identified only in strains expressing SPA-tagged ACPs but not PAO1 were considered potential ACP-binding partners. For the most part, the three ACPs have different sets of binding partners, commensurate with distinct physiological roles for these proteins. For AcpP, 10 protein candidates were identified (**Table 2**), including FabG, FabZ, FabA, GlmU, IscS, and LpxD, which are known to bind *E. coli* ACP (Butland et al., 2005). Their identification in *P. aeruginosa* provides further evidence that AcpP is functionally equivalent to *E. coli* ACP (Ma et al., 2017). Interactions with the Type II FAS enzymes FabG, FabZ, and FabA are consistent with a role for AcpP in fatty acid biosynthesis. New binding partners of AcpP were also found compared to those known for *E. coli* ACP, including CobL, LipB, SpeE2, and AlgB. One interaction that was expected but not observed was

that between AcpP and SpoT, because these are known to form a complex in *P. aeruginosa* (Battesti and Bouveret, 2009).

Only four binding partners of Acp1 were identified: PepA, GlpR, Tuf1, and FabG (**Table 2**). PepA is a leucine aminopeptidase that is homologous to *E. coli* PepA (Woolwine and Wozniak, 1999), GlpR is annotated as a repressor of the glycerol-3-phosphate regulon and Tuf1 as the elongation factor Tu (Winsor et al., 2016). One reason for there being fewer binding partners for Acp1 compared to AcpP or Acp3 might be the relatively lower expression of the protein at selected sampling time of 12 h (see **Figure 1B**).

Ten protein-binding partners of Acp3 were identified and most are enzymes of various functions (**Table 2**). The observed binding with IscS, GlmU, and FabG is in common with AcpP. Of the other proteins identified, novel binding partners include the 3-oxo-acyl-ACP synthase, FabH2 (PA3333), and also PqsD. *fabH2* is located within one putative operon with *acp3* (PA3334) and is of unknown function, in contrast to FabH (PA5814), which initiates fatty acid biosynthesis in *P. aeruginosa* (Zhang and Rock, 2012). PqsD is essential for the production of the quinolones DHQ and alkyl quinolones (Zhang et al., 2008). Additional partners are ArcB, an ornithine carbamoyltransferase, SucC, which is involved in the biosynthesis of succinate (Kapatral et al., 2000), and Fur, which is a ferric uptake regulator (Ochsner et al., 1995). Finally, KatA, which is the major catalase in *P. aeruginosa*, was identified as a binding partner of Acp3 and this was investigated further (see below).

## Interaction of KatA and Acp3 by Pull-Down Assay

One of the most intriguing binding hits for Acp3 was KatA, which is the major catalase in *P. aeruginosa* and is required for resistance to peroxide and osmotic stress (Lee et al., 2005). To confirm that

**TABLE 2 |** Binding partners of ACPs in *P. aeruginosa* identified by tandem affinity purification.

| Locus | Protein | Function | SC[a] | SC | Abundance[b] | p-Value[c] |
|---|---|---|---|---|---|---|
| **AcpP** | | | **PAO1** | **CW20** | | |
| PA2967 | FabG | 3-Oxo-acyl-ACP reductase | 0 | 174 | 340.24 | 2.14E−54 |
| PA3645 | FabZ | 3-Hydroxyacyl-ACP dehydratase | 0 | 53 | 158.08 | 1.02E−17 |
| PA2907 | CobL | Precorrin-6YC(5,15)-methyltransferase | 0 | 121 | 137.18 | 2.31E−38 |
| PA5552 | GlmU | Bifunctional enzyme of LPS/peptidoglycan synthesis | 0 | 119 | 121.87 | 9.31E−38 |
| PA1610 | FabA | 3-Hydroxydecanoyl-ACP dehydratase | 0 | 22 | 58 | 3.35E−08 |
| PA3814 | IscS | Cysteine desulfurase | 0 | 24 | 26.88 | 8.03E−09 |
| PA3997 | LipB | Octanoyltransferase | 0 | 6 | 12.58 | 3.93E−03 |
| PA4774 | SpeE2 | Spermidine synthase 2 | 0 | 6 | 7.59 | 3.93E−03 |
| PA3646 | LpxD | UDP-3-O-acylglucosamine N-acyltransferase | 0 | 5 | 6.91 | 8.47E−03 |
| PA5483 | AlgB | Alginate biosynthesis transcriptional regulator | 0 | 6 | 6.09 | 0.00393 |
| **Acp1** | | | **PAO1** | **CW22** | | |
| PA3831 | PepA | Cytosol aminopeptidase | 0 | 49 | 46 | 1.70E−16 |
| PA3583 | GlpR | Glycerol-3-phosphate regulon repressor | 0 | 23 | 41 | 1.64E−08 |
| PA2967 | FabG | 3-Oxo-acyl-ACP reductase | 0 | 8 | 15.6 | 8.68E−04 |
| PA4277 | Tuf1 | Elongation factor Tu | 0 | 13 | 15 | 2.19E−05 |
| **Acp3** | | | **PAO1** | **CW21** | | |
| PA3814 | IscS | Cysteine desulfurase | 0 | 69 | 77.29 | 1.37E−22 |
| PA3333 | FabH2 | 3-Oxo-acyl-ACP synthase | 0 | 49 | 72.09 | 1.70E−16 |
| PA4236 | KatA | Catalase | 0 | 64 | 57.6 | 4.55E−21 |
| PA5172 | ArcB | Ornithine carbamoyltransferase | 0 | 30 | 39.39 | 1.13E−10 |
| PA4764 | Fur | Ferric uptake regulation protein | 0 | 8 | 26.27 | 8.69E−04 |
| PA2967 | FabG | 3-Oxo-acyl-ACP reductase | 0 | 11 | 21.51 | 9.43E−05 |
| PA1588 | SucC | Succinyl-CoA ligase | 0 | 11 | 13.25 | 9.43E−05 |
| PA4740 | Pnp | Polyribonucleotide nucleotidyltransferase | 0 | 17 | 11.27 | 1.21E−06 |
| PA0999 | PqsD | PQS biosynthetic protein | 0 | 8 | 11 | 8.69E−04 |
| PA5552 | GlmU | Bifunctional protein | 0 | 7 | 7.17 | 1.84E−03 |

[a]SC is the summed number of spectral counts (i.e., MS/MS scans) assigned to one identified protein, used as a semi-quantitative index for protein abundance. [b]Abundance = SC × 50 (kDa)/protein size (kDa). Proteins are listed with abundance above 5. [c]p-Value less than 0.05 indicates significant change. The p value is derived by the G-test (Zhou et al., 2010).

Acp3 and KatA interact with each other, we performed a reverse pull-down assay in which the pEXHTB plasmid expressing His-tagged KatA was transformed into PAO1 expressing FLAG-tagged Acp3 (CW21/pEXHTB-katA). The immunoblot shows that the FLAG-tagged Acp3 co-eluted with His-tagged KatA from the $Ni^{2+}$-affinity column (**Figure 3**, right panel). The same strain transformed with vector expressing just the His tag was used as a comparison control (CW21/pEXHTB), and no Acp3 was detected in the eluate (**Figure 3**, left panel). This experiment confirms that Acp3 binds KatA specifically.

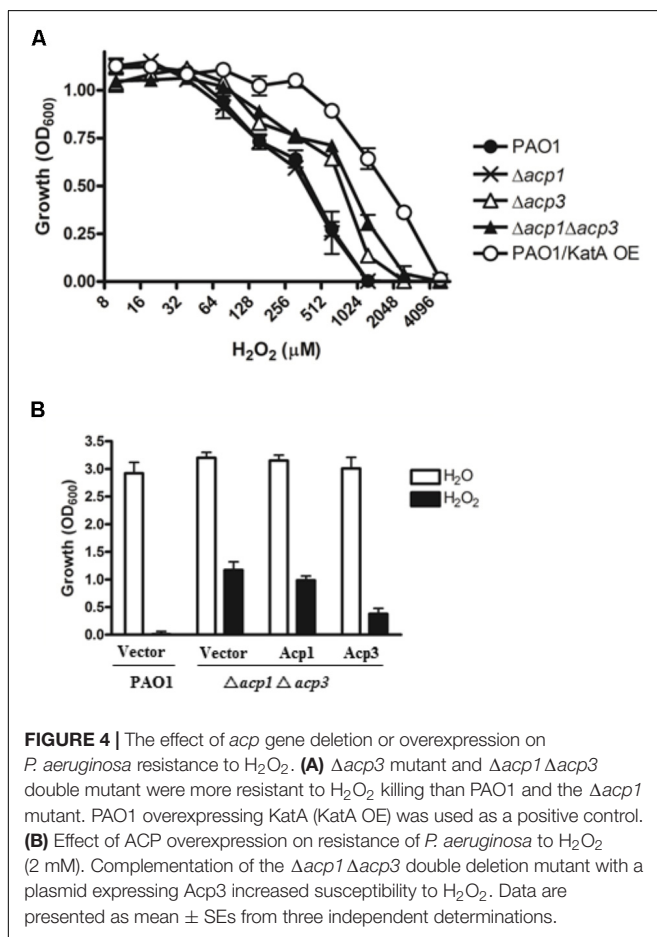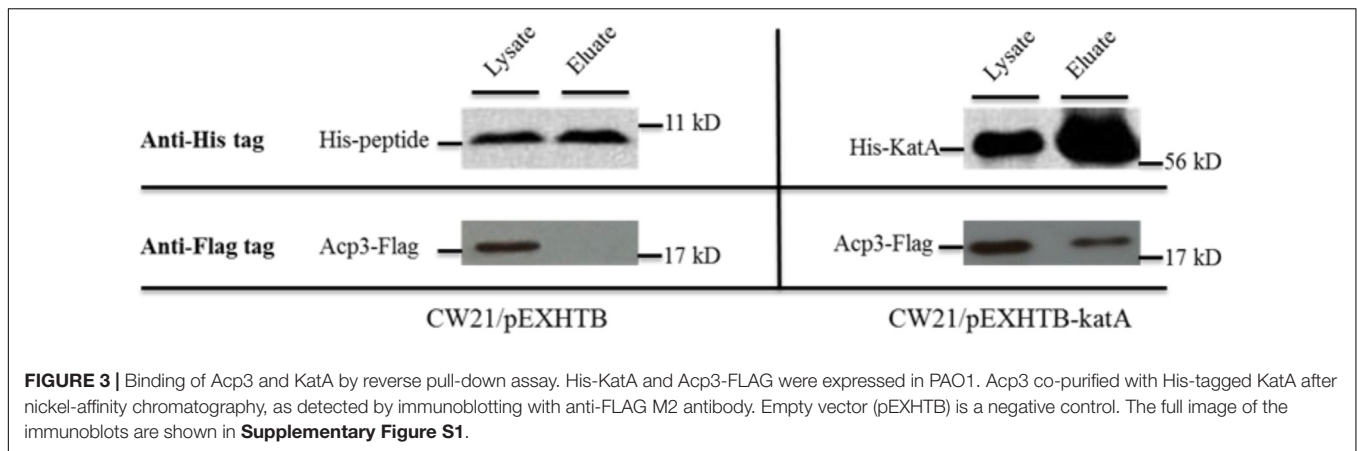## *acp3* Mutant Is More Resistant to Hydrogen Peroxide

One reason for the higher persistence of the *acp3* mutant in the mouse infection model could be increased tolerance to reaction oxygen species (ROS) related to the binding of Acp3 with KatA and potential influence on its activity. To examine this, we determined the $H_2O_2$ resistance of the *acp* mutants. Both the $\Delta acp3$ and $\Delta acp1/\Delta acp3$ mutants exhibited a twofold higher resistance to killing by $H_2O_2$, compared with PAO1 (**Figure 4A**). The $\Delta acp1$ mutant exhibited similar susceptibility as wild type. As a positive control, overexpression of KatA increased resistance in PAO1 by fourfold. To confirm the effect of *acp* deletion on

$H_2O_2$ resistance, we complemented the $\Delta acp1/\Delta acp3$ mutant strain with plasmids expressing Acp1 or Acp3. When Acp3 was expressed, susceptibility of the strain to $H_2O_2$ was increased, whereas expression of Acp1 had little effect compared to the vector control (**Figure 4B**). These data show that the presence of Acp3 increases susceptibility of *P. aeruginosa* to $H_2O_2$.

## Acp3 Represses the Catalase Activity of KatA

Since catalases play a major role in protecting bacteria against ROS *via* decomposition of $H_2O_2$ (Mishra and Imlay, 2012), we measured the catalase activity of the *acp1* and *acp3* deletion strains by the ferrous oxidation xylenol orange (FOX) assay (Ou and Wolff, 1996). Compared with the wild-type PAO1 strain, deletion of *acp3* enhanced the catalase activity of *P. aeruginosa* by 50%, with a lesser increase observed in the *acp1* deletion strain (**Figure 5**). Complementation of Acp3 in the $\Delta acp1/\Delta acp3$ double mutants reduced catalase activity back to wild-type levels. These data are consistent with Acp3 acting as a repressor of KatA activity.

To explore the functional relationship between Acp3 and KatA further, we deleted the *katA* gene in wild-type and *acp* mutants. Deletion of *katA* in PAO1 resulted in a nearly 300-fold reduction

**FIGURE 3 |** Binding of Acp3 and KatA by reverse pull-down assay. His-KatA and Acp3-FLAG were expressed in PAO1. Acp3 co-purified with His-tagged KatA after nickel-affinity chromatography, as detected by immunoblotting with anti-FLAG M2 antibody. Empty vector (pEXHTB) is a negative control. The full image of the immunoblots are shown in **Supplementary Figure S1**.



**FIGURE 4 |** The effect of *acp* gene deletion or overexpression on *P. aeruginosa* resistance to $H_2O_2$. **(A)** $\Delta acp3$ mutant and $\Delta acp1\Delta acp3$ double mutant were more resistant to $H_2O_2$ killing than PAO1 and the $\Delta acp1$ mutant. PAO1 overexpressing KatA (KatA OE) was used as a positive control. **(B)** Effect of ACP overexpression on resistance of *P. aeruginosa* to $H_2O_2$ (2 mM). Complementation of the $\Delta acp1\Delta acp3$ double deletion mutant with a plasmid expressing Acp3 increased susceptibility to $H_2O_2$. Data are presented as mean ± SEs from three independent determinations.



**FIGURE 5 |** The absence of Acp3 increases the catalase activity of *P. aeruginosa*. $\Delta acp3$ and $\Delta acp1\Delta acp3$ mutants exhibited higher catalase activity than wild-type PAO1. Catalase activity reduced after plasmids expressing Acp1 and Acp3 were introduced back into the $\Delta acp1\Delta acp3$ mutant. Data are presented as mean ± SEs from three independent experiments. Student's *t*-test was performed between PAO1 and *acp* mutants. * indicates $p < 0.01$.

in catalase activity (data not shown). Importantly, there was no difference in catalase activity or resistance to $H_2O_2$ between the $\Delta katA$ and $\Delta acp3/\Delta katA$ strains (**Figure 6**). This shows that the $H_2O_2$ resistance of the *acp3* mutant is mediated through KatA.
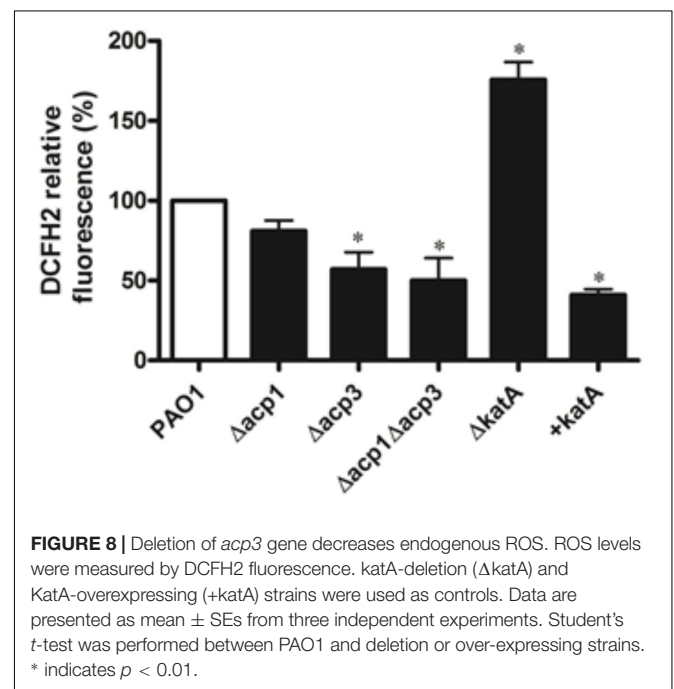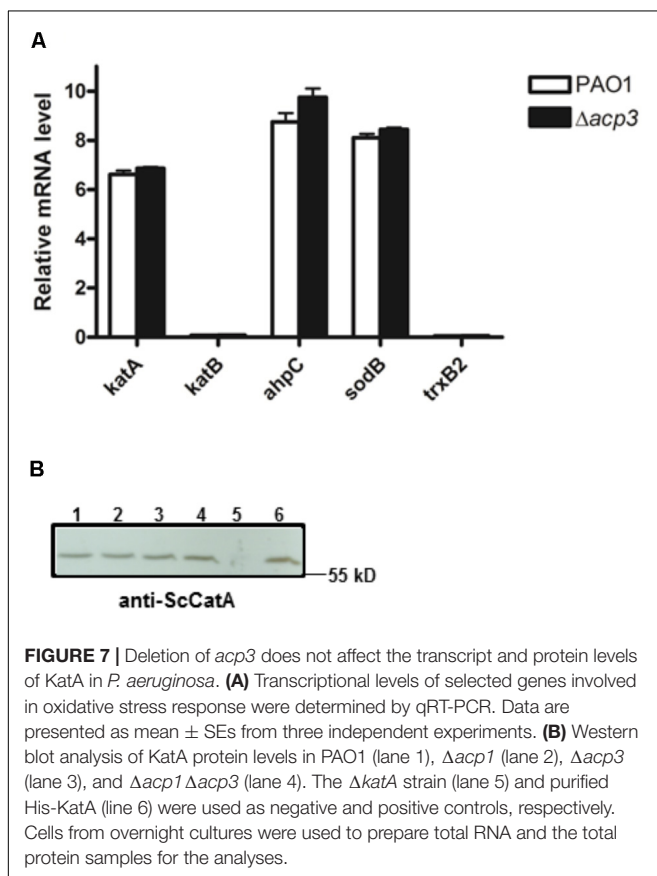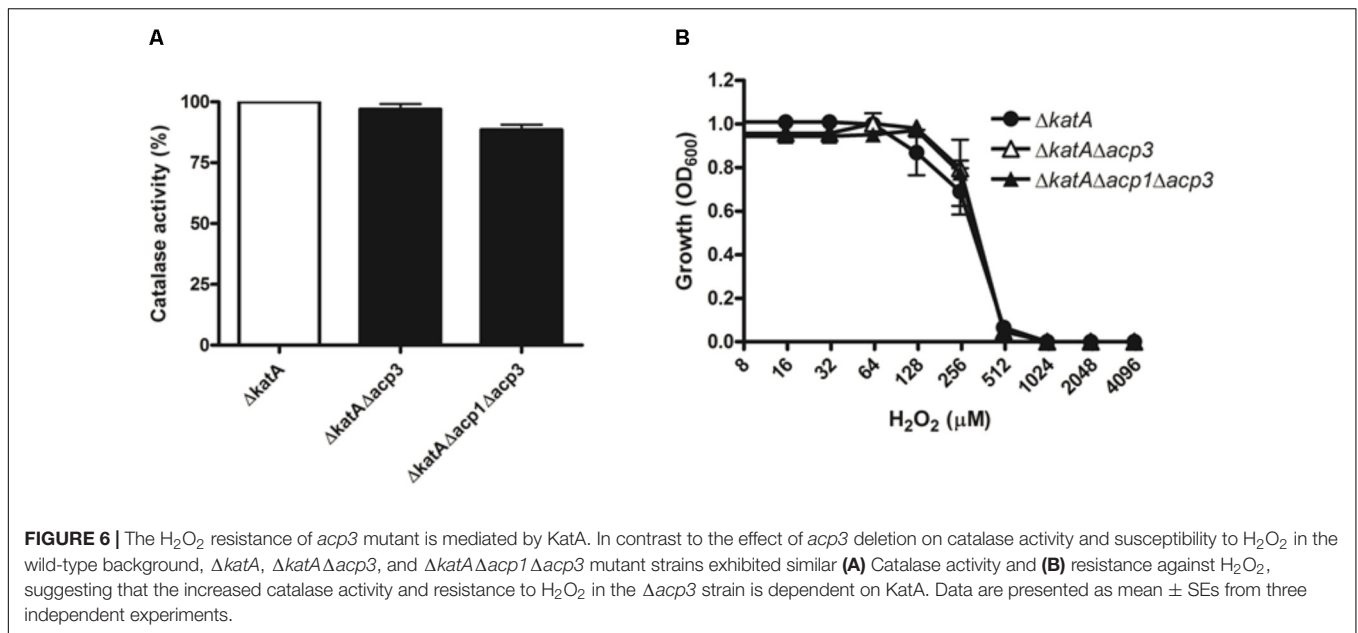
To address whether the absence of Acp3 affects the expression level of *katA*, we measured the level of *katA* transcript in the *acp3* deletion strain, as well as for several genes that respond to oxidative stress, specifically *katB*, *ahpC*, *sodB*, and *trxB2*
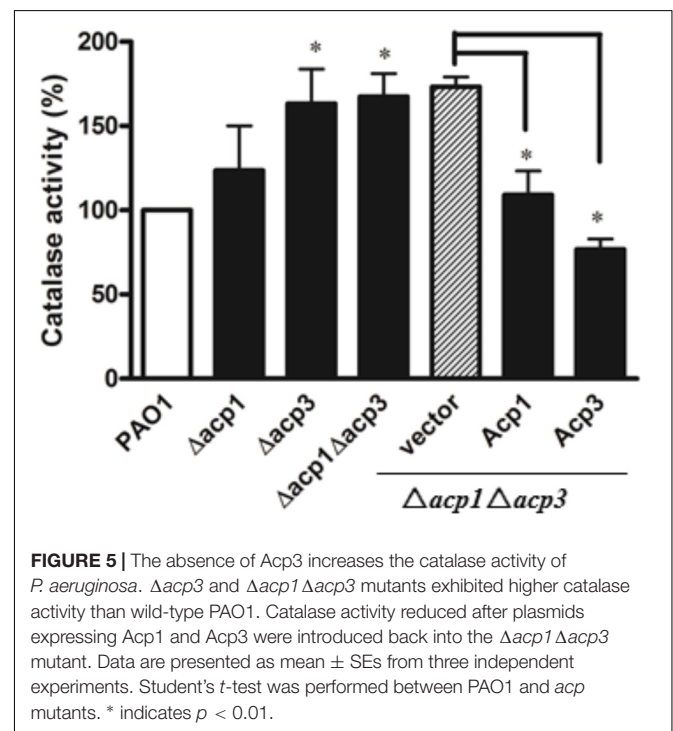
(Salunkhe et al., 2005). Compared to PAO1, deletion of *acp3* did not alter transcription levels of *katA* or any of the other selected genes (**Figure 7A**). Similarly, protein levels of KatA were the same in *acp1* or *acp3* deletion strains compared to PAO1 (**Figure 7B**). These data suggest that the activity of KatA is inhibited by a direct interaction with Acp3 and not by transcriptional or translational regulation.

## Deletion of *acp3* Reduces Endogenous ROS Levels

To determine whether inhibition of KatA activity by Acp3 correlates with levels of endogenous ROS, we used DCFH₂, a non-specific fluorescence probe, to measure ROS levels in *P. aeruginosa* cells (Brömme et al., 2008). Significantly less ROS

**FIGURE 6 |** The $H_2O_2$ resistance of *acp3* mutant is mediated by KatA. In contrast to the effect of *acp3* deletion on catalase activity and susceptibility to $H_2O_2$ in the wild-type background, $\Delta katA$, $\Delta katA\Delta acp3$, and $\Delta katA\Delta acp1\Delta acp3$ mutant strains exhibited similar **(A)** Catalase activity and **(B)** resistance against $H_2O_2$, suggesting that the increased catalase activity and resistance to $H_2O_2$ in the $\Delta acp3$ strain is dependent on KatA. Data are presented as mean ± SEs from three independent experiments.



**FIGURE 7 |** Deletion of *acp3* does not affect the transcript and protein levels of KatA in *P. aeruginosa*. **(A)** Transcriptional levels of selected genes involved in oxidative stress response were determined by qRT-PCR. Data are presented as mean ± SEs from three independent experiments. **(B)** Western blot analysis of KatA protein levels in PAO1 (lane 1), $\Delta acp1$ (lane 2), $\Delta acp3$ (lane 3), and $\Delta acp1\Delta acp3$ (lane 4). The $\Delta katA$ strain (lane 5) and purified His-KatA (line 6) were used as negative and positive controls, respectively. Cells from overnight cultures were used to prepare total RNA and the total protein samples for the analyses.



**FIGURE 8 |** Deletion of *acp3* gene decreases endogenous ROS. ROS levels were measured by DCFH2 fluorescence. katA-deletion ($\Delta katA$) and KatA-overexpressing (+katA) strains were used as controls. Data are presented as mean ± SEs from three independent experiments. Student's *t*-test was performed between PAO1 and deletion or over-expressing strains. * indicates $p < 0.01$.

was detected in the $\Delta acp3$ mutant compared with wild type, commensurate with a higher level of KatA activity (**Figure 8**). In addition, the *katA* deletion mutant contained a much higher level of ROS and the KatA overexpression strain exhibited lower ROS. These data suggest that release of KatA inhibition by the *acp3* deletion decreases ROS levels in *P. aeruginosa*.

## DISCUSSION

In addition to canonical ACPs that function during FAS, bacteria typically express other ACPs and in many cases, the functions of these homologues are unknown. Following a recent study in which AcpP was confirmed as the essential ACP involved in membrane FAS (Ma et al., 2017), we investigated Acp1 and Acp3

of *P. aeruginosa* in order to shed light on their physiological roles in this important pathogen. The major finding is that Acp3 impacts virulence and *in vivo* pathogenicity of *P. aeruginosa* and also appears to regulate the activity of the catalase KatA in a way that suggests involvement in the cellular response to oxidative stress.

In keeping with the idea that Acp1 or Acp3 have a role in pathogenesis, we first investigated whether their expression is regulated by QS. This is an important mechanism employed by bacterial populations to respond to environmental cues, such as nutrient restriction or the presence of antibiotics. In *P. aeruginosa*, QS governs biofilm formation, swarming motility, and production of virulence factors such as pyocyanin, elastases, and rhamnolipids (Venturi, 2006). A connection between ACPs and QS is logical because the synthesis of QS signals such as PQS and acyl homoserine lactones (HSLs) requires acyl ACP (Parsek et al., 1997; Raychaudhuri et al., 2005; Dulcey et al., 2013). Furthermore, the higher levels of both transcripts and proteins for ACPs observed during the transition of cell cultures from log to stationary phase could involve QS. Accordingly, we found that levels of *acp1* and *acp3* transcripts are significantly lower in *P. aeruginosa* strains lacking LasR or RhlR, which are the receptors for 3-oxo-C12-HSL and C4-HSL, respectively (Gambello and Iglewski, 1991; Ochsner and Reiser, 1995) and thus suggests that expression of Acp1 and Acp3 is governed by the QS machinery.

Our next step was to assess whether Acp1 or Acp3 plays a role in pathogenicity. We found that deletion of *acp1* or acp3 has no effect on *in vitro* virulence of *P. aeruginosa*, except for thicker biofilm. By contrast, when tested in a mouse infection model, a 1000-fold increase in bacterial load was detected for both *acp1* and *acp3* deletion mutants, indicating that both Acp1 and Acp3 play a role in *P. aeruginosa* pathogenicity *in vivo*. A previous study showed increased expression levels of both *acp1* and *acp3* genes in acute and chronic wound infection models in mice (Turner et al., 2014), suggesting that Acp1 and Acp3 are important for *P. aeruginosa* fitness in a disease environment *in vivo*. The different effects of *acp1* and *acp3* deletion on virulence *in vitro* versus *in vivo* may be due to the differences in the availability of nutrients and oxygen in the growth environment.

To probe their physiological roles further, we used TAP (Babu et al., 2009) to identify protein-binding partners of Acp1 and Acp3. The identification of several enzymes involved in fatty acid biosynthesis as binding partners of AcpP provided validation for the experiment. Acp1 and Acp3 also bound some enzymes of Type II FAS, but more so to proteins from other areas of metabolism. For instance, the top hit for Acp1 was PepA (also known as PhpA), which possesses aminopeptidase activity and whose disruption in an *algB* mutant increases alginate expression in *P. aeruginosa* (Woolwine and Wozniak, 1999). PepA also plays a role within the Xer recombinase system of *E. coli* (where it is called XerB) (Stirling et al., 1989) and it lowers expression of carbamoyl phosphate synthase by binding to the promoter region of the *carAB* operon in *E. coli* (Charlier et al., 1995). The association of PepA with Acp1 adds a further dimension to a protein

that appears to function in several very different processes. Another binding hit for Acp1 is GlpR, which is a repressor of genes involved in glycerol metabolism (Schweizer and Po, 1996). Since genetic deletion of GlpR increases biofilm formation in *P. aeruginosa* (Scoffield and Silo-Suh, 2016), it is tempting to speculate that its association with Acp1 may affect virulence.

Among the proteins that bound Acp3 were IscS, FabH2, KatA, and ArcB. The breadth and diversity of these interactions hints at the versatility of Acp3 in its functions. The top hit was IscS, a cysteine desulfurase that provides sulfur for the biosynthesis of FeS clusters, thiamine, biotin, lipoic acid, modified nucleosides in tRNAs, and the molybdenum cofactor (Moco), among others (Hidese et al., 2011; Leimkuhler et al., 2017). Its interaction with Acp3 is not the first evidence of a functional association between ACPs and cysteine desulfurases. Using the same TAP approach, *E. coli* ACP was also found to bind IscS, with the interaction mediated by a disulfide bond between the 4-phosphopantetheine group and Cys328 of IscS (Gully et al., 2003). It remains to be established whether this group is also required for the interaction in *P. aeruginosa*.

Interactions between IscS and ACP also occur in humans, albeit indirectly. A multisubunit complex containing NFS1 (the name given to IscS in humans, which shares ∼60% amino acid sequence identity with *E. coli* IscS), the LYR protein ISD11 and acyl ACP assembles FeS clusters in mitochondria (Van Vranken et al., 2016). Within this complex, ACP interacts with the ISD11 subunit (Herrera et al., 2018), which in turn interacts with NSF1 (Cory et al., 2017). Such Acp–IscS interactions in other species supports the idea that Acp3 may have a role in assembly of FeS clusters in *P. aeruginosa*.

Another putative binding partner for Acp3 is ArcB, an ornithine carbamoyl transferase (OCT). This enzyme is part of the arginine deiminase system (ADS) found in bacteria that allows anaerobic growth on arginine. In *P. aeruginosa*, OCT is a dodecameric complex of identical protomers (Marcq et al., 1991) and is allosterically inhibited by spermidine and activated by AMP regulation (Tricot et al., 1993). There appears no involvement of ACP in the reaction mechanism (Tricot et al., 1998) and this putative interaction therefore requires further investigation.

The apparent promiscuity in binding of *P. aeruginosa* ACPs and especially those for Acp3 is mirrored by *E. coli* ACP, which binds to a number of protein factors outside of its canonical function in FAS, including IscS, MukB, YbgC, and SpoT (Gully et al., 2003; Gully and Bouveret, 2006). Of these, the interaction with SpoT has been examined in most detail (Battesti and Bouveret, 2006; Angelini et al., 2012). SpoT is a factor that changes its activity from (p)ppGpp hydrolysis to (p)ppGpp synthesis in response to starvation signals, leading to initiation of the stringent response. It has been postulated that the switch in its enzymatic activity toward synthesis may be governed by the binding of ACP to the C-terminal domain of SpoT (Battesti and Bouveret, 2006). Mutations that abrogate binding to SpoT mostly map to hydrophobic residues in helix II of ACP (Angelini et al., 2012) and this region of the protein also mediates interactions with its other protein partners, including FabI, AcpS, and YchM

(Parris et al., 2000; Rafi et al., 2006; Babu et al., 2010). Each of the new potential binding partners revealed here for Acp1 and Acp3 offers opportunity to investigate the molecular details of these interactions in a similar way as ACP-SpoT, including establishing whether helix II is a common interface, determining whether an acylated 4-phosphopantetheine prosthetic group is involved in the binding, and understanding their physiological consequences in *P. aeruginosa*.

With this goal in mind, we decided to investigate further the interaction of Acp3 with KatA, the major catalase of *P. aeruginosa* (Hassett et al., 1992). *katA* is one of the oxidative stress response genes expressed during aerobic metabolism or in response to exogenous ROS, and its expression is controlled by the global transcriptional regulator OxyR (Heo et al., 2010). At first sight, the reason for an interaction between Acp3 and KatA is not obvious, but can be rationalized in the context of cellular responses of *P. aeruginosa* to oxidative stress. Under such conditions, KatA is upregulated in order to dismutate $H_2O_2$ and other ROS, and presumably is negatively regulated when ROS levels normalize. It appears that by binding to KatA, Acp3 acts as a negative regulator of its catalase activity. This is supported by the increased resistance of the *acp3* deletion strain to $H_2O_2$ (because KatA activity is constitutively higher without Acp3). Higher tolerance to ROS may also explain the increased persistence of the *acp3* deletion mutant *in vivo*. The inhibition of KatA by binding of Acp3 is reminiscent of the ACP-SpoT interaction and a further example of how ACPs can regulate enzyme activities.

It is interesting to note that the putative interaction between Acp3 and IscC mentioned above may also be related to oxidative stress. This is because a strain of *C. difficile* lacking IscS2 (the homologue of IscS) fails to grow when oxygen levels go above 2% (Giordano et al., 2018) suggesting it protects against oxidative stress. However, it needs to be established whether binding of Acp3 to IscS represses its cysteine desulfurase activity similar to KatA, or whether it enhances activity.

Why Acp3 regulates the activity of KatA is unknown. There are probably several potential reasons that could be invoked, but one intriguing possibility relates to the so-called "Insurance Hypothesis." This is the diversification of phenotype in bacterial communities in response to harsh conditions (Boles et al., 2004). The increased expression of Acp3 prior to stationary phase may serve to reduce catalase activity and thereby increase ROS levels. The subsequent DNA damage and mutation would increase genotypic and phenotypic diversity within the biofilm (Boles et al., 2004), thus allowing the community to survive. While more work is needed to uncover its details, the observed binding of Acp3 to KatA reveals an additional mechanism of control within an already complex regulatory network for KatA and a potential role for this ACP in response to oxidative stress.

## AUTHOR CONTRIBUTIONS

WC generated all strains for this work, performed the phenotype analyses and enzymatic assays *in vitro*, prepared the figures, and contributed to the writing of the manuscript. BW and JG performed the *in vivo* pathogenicity assays. Y-MZ conceived the study, directed the experiments, and helped draft the manuscript. CD contributed ideas to the project and helped draft the manuscript. All authors contributed to the analysis and interpretation of data. All authors approved the manuscript submitted.

## FUNDING

## ACKNOWLEDGMENTS

## SUPPLEMENTARY MATERIAL

The Supplementary Material for this article can be found online at: https://www.frontiersin.org/articles/10.3389/fmicb.2018.02244/full#supplementary-material

## REFERENCES

Angelini, S., My, L., and Bouveret, E. (2012). Disrupting the Acyl carrier protein/SpoT interaction *in vivo*: identification of ACP residues involved in the interaction and consequence on growth. *PLoS One* 7:e36111. doi: 10.1371/journal.pone.0036111

Babu, M., Butland, G., Pogoutse, O., Li, J., Greenblatt, J. F., and Emili, A. (2009). Sequential peptide affinity purification system for the systematic isolation and identification of protein complexes from *Escherichia coli*. *Methods Mol. Biol.* 564, 373–400. doi: 10.1007/978-1-60761-157-8-22

Babu, M., Greenblatt, J. F., Emili, A., Strynadka, N. C., Reithmeier, R. A., and Moraes, T. F. (2010). Structure of a SLC26 anion transporter STAS domain in complex with acyl carrier protein: implications for *E. coli* YchM in fatty acid metabolism. *Structure* 18, 1450–1462. doi: 10.1016/j.str.2010.08.015

Battesti, A., and Bouveret, E. (2006). Acyl carrier protein/SpoT interaction, the switch linking SpoT-dependent stress response to fatty acid metabolism. *Mol. Microbiol.* 62, 1048–1063. doi: 10.1111/j.1365-2958.2006.05442.x

Battesti, A., and Bouveret, E. (2009). Bacteria possessing two RelA/SpoT-like proteins have evolved a specific stringent response involving the acyl carrier protein-SpoT interaction. *J. Bacteriol.* 191, 616–624. doi: 10.1128/JB.01195-08

Boles, B. R., Thoendel, M., and Singh, P. K. (2004). Self-generated diversity produces "insurance effects" in biofilm communities. *Proc. Natl. Acad. Sci. U.S.A.* 101, 16630–16635. doi: 10.1073/pnas.0407460101

Brömme, H.-J., Zühlke, L., Silber, R.-E., and Simm, A. (2008). DCFH2 interactions with hydroxyl radicals and other oxidants – Influence of organic solvents. *Exp. Gerontol.* 43, 638–644. doi: 10.1016/j.exger.2008.01.010

Brozek, K. A., Carlson, R., and Wand Raetz, C. R. (1996). A special acyl carrier protein for transferring long hydroxylated fatty acids to lipid A in *Rhizobium*. *J. Biol. Chem.* 271, 32126–32136. doi: 10.1074/jbc.271.50.32126

Butland, G., Peregrin-Alvarez, J. M., Li, J., Yang, W., Yang, X., Canadien, V., et al. (2005). Interaction network containing conserved and essential protein complexes in *Escherichia coli*. *Nature* 433, 531–537. doi: 10.1038/nature03239

Byers, D., and Gong, M. H. (2007). Acyl carrier protein: structure-function relationships in a conserved multifunctional protein family. *Biochem. Cell Biol.* 85, 649–662. doi: 10.1139/o07-109

Chan, D. I., and Vogel, H. J. (2010). Current understanding of fatty acid biosynthesis and the acyl carrier protein. *Biochem. J.* 430, 1–19. doi: 10.1042/BJ20100462

Charlier, D., Hassanzadeh, G., Kholti, A., Gigot, D., Pierard, A., and Glansdorff, N. (1995). carP, involved in pyrimidine regulation of the *Escherichia coli* carbamoylphosphate synthetase operon encodes a sequence-specific DNA-binding protein identical to XerB and PepA, also required for resolution of ColEI multimers. *J. Mol. Biol.* 250, 392–406. doi: 10.1006/jmbi.1995.0385

Choi, K. H., and Schweizer, H. P. (2005). An improved method for rapid generation of unmarked *Pseudomonas aeruginosa* deletion mutants. *BMC Microbiol.* 5:30. doi: 10.1186/1471-2180-5-30

Chugani, S., Kim, B. S., Phattarasukol, S., Brittnacher, M. J., Choi, S. H., Harwood, C. S., et al. (2012). Strain-dependent diversity in the *Pseudomonas aeruginosa* quorum-sensing regulon. *Proc. Natl. Acad. Sci. U.S.A.* 109, E2823–E2831. doi: 10.1073/pnas.1214128109

Cory, S. A., Van Vranken, J. G., Brignole, E. J., Patra, S., Winge, D. R., Drennan, C. L., et al. (2017). Structure of human Fe-S assembly subcomplex reveals unexpected cysteine desulfurase architecture and acyl-ACP-ISD11 interactions. *Proc. Natl. Acad. Sci. U.S.A.* 114, E5325–E5334. doi: 10.1073/pnas.1702849114

De Lay, N. R., and Cronan, J. E. (2007). *In vivo* functional analyses of the type II acyl carrier proteins of fatty acid biosynthesis. *J. Biol. Chem.* 282, 20319–20328. doi: 10.1074/jbc.M703789200

de Lorenzo, V., and Timmis, K. N. (1994). Analysis and construction of stable phenotypes in gram-negative bacteria with Tn5- and Tn10-derived minitransposons. *Methods Enzymol.* 235, 386–405. doi: 10.1016/0076-6879(94)35157-0

Dulcey, C. E., Dekimpe, V., Fauvelle, D. A., Milot, S., Groleau, M. C., Doucet, N., et al. (2013). The end of an old hypothesis: the *Pseudomonas* signaling molecules 4-hydroxy-2-alkylquinolines derive from fatty acids, not 3-ketofatty acids. *Chem. Biol.* 20, 1481–1491. doi: 10.1016/j.chembiol.2013.09.021

Epple, G., van der Drift, K. M., Thomas-Oates, J. E., and Geiger, O. (1998). Characterization of a novel acyl carrier protein, RkpF, encoded by an operon involved in capsular polysaccharide biosynthesis in *Sinorhizobium meliloti*. *J. Bacteriol.* 180, 4950–4954.

Gambello, M. J., and Iglewski, B. H. (1991). Cloning and characterization of the *Pseudomonas aeruginosa* lasR gene, a transcriptional activator of elastase expression. *J. Bacteriol.* 173, 3000–3009. doi: 10.1128/jb.173.9.3000-3009.1991

Geiger, O., and Lopez-Lara, I. M. (2002). Rhizobial acyl carrier proteins and their roles in the formation of bacterial cell-surface components that are required for the development of nitrogen-fixing root nodules on legume hosts. *FEMS Microbiol. Lett.* 208, 153–162. doi: 10.1111/j.1574-6968.2002.tb11075.x

Geiger, O., Spaink, H. P., and Kennedy, E. P. (1991). Isolation of the *Rhizobium leguminosarum* NodF nodulation protein: NodF carries a 4'-phosphopantetheine prosthetic group. *J. Bacteriol.* 173, 2872–2878. doi: 10.1128/jb.173.9.2872-2878.1991

Giordano, N., Hastie, J. L., Smith, A. D., Foss, E. D., Gutierrez-Munoz, D. F., and Carlson, P. E. Jr. (2018). Cysteine desulfurase IscS2 plays a role in oxygen resistance in clostridium difficile. *Infect. Immun.* 86, e326–e318. doi: 10.1128/IAI.00326-18

Govan, J. R., and Deretic, V. (1996). Microbial pathogenesis in cystic fibrosis: mucoid *Pseudomonas aeruginosa* and *Burkholderia cepacia*. *Microbiol. Rev.* 60, 539–574.

Gruber, J. D., Chen, W., Parnham, S., Beauchesne, K., Moeller, P., Flume, P. A., et al. (2016). The role of 2,4-dihydroxyquinoline (DHQ) in *Pseudomonas aeruginosa* pathogenicity. *PeerJ* 4:e1495. doi: 10.7717/peerj.1495

Gully, D., and Bouveret, E. (2006). A protein network for phospholipid synthesis uncovered by a variant of the tandem affinity purification method in *Escherichia coli*. *Proteomics* 6, 282–293. doi: 10.1002/pmic.200500115

Gully, D., Moinier, D., Loiseau, L., and Bouveret, E. (2003). New partners of acyl carrier protein detected in *Escherichia coli* by tandem affinity purification. *FEBS Lett.* 548, 90–96. doi: 10.1016/S0014-5793(03)00746-4

Haag, A. F., Wehmeier, S., Beck, S., Marlow, V. L., Fletcher, V., James, E. K., et al. (2009). The *Sinorhizobium meliloti* LpxXL and AcpXL proteins play important roles in bacteroid development within alfalfa. *J. Bacteriol.* 191, 4681–4686. doi: 10.1128/JB.00318-09

Hassett, D. J., Charniga, L., Bean, K., Ohman, D. E., and Cohen, M. S. (1992). Response of *Pseudomonas aeruginosa* to pyocyanin: mechanisms of resistance, antioxidant defenses, and demonstration of a manganese-cofactored superoxide dismutase. *Infect. Immun.* 60, 328–336.

Hentzer, M., Wu, H., Andersen, J. B., Riedel, K., Rasmussen, T. B., Bagge, N., et al. (2003). Attenuation of *Pseudomonas aeruginosa* virulence by quorum sensing inhibitors. *EMBO J.* 22, 3803–3815. doi: 10.1093/emboj/cdg366

Heo, Y. J., Chung, I. Y., Cho, W. J., Lee, B. Y., Kim, J. H., Choi, K. H., et al. (2010). The major catalase gene (katA) of *Pseudomonas aeruginosa* PA14 is under both positive and negative control of the global transactivator OxyR in response to hydrogen peroxide. *J. Bacteriol.* 192, 381–390. doi: 10.1128/JB.00980-09

Herrera, M. G., Pignataro, M. F., Noguera, M. E., Cruz, K. M., and Santos, J. (2018). Rescuing the rescuer: on the protein complex between the human mitochondrial Acyl carrier protein and ISD11. *ACS Chem. Biol.* 13, 1455–1462. doi: 10.1021/acschembio.8b00184

Hidese, R., Mihara, H., and Esaki, N. (2011). Bacterial cysteine desulfurases: versatile key players in biosynthetic pathways of sulfur-containing biofactors. *Appl. Microbiol. Biotechnol.* 91, 47–61. doi: 10.1007/s00253-011-3336-x

Holloway, B. W., Krishnapillai, V., and Morgan, A. F. (1979). Chromosomal genetics of *Pseudomonas*. *Microbiol. Rev.* 43, 73–102.

Kapatral, V., Bina, X., and Chakrabarty, A. M. (2000). Succinyl coenzyme A synthetase of *Pseudomonas aeruginosa* with a broad specificity for nucleoside triphosphate (NTP) synthesis modulates specificity for NTP synthesis by the 12-kilodalton form of nucleoside diphosphate kinase. *J. Bacteriol.* 182, 1333–1339. doi: 10.1128/JB.182.5.1333-1339.2000

Lee, J. S., Heo, Y. J., Lee, J. K., and Cho, Y. H. (2005). KatA, the major catalase, is critical for osmoprotection and virulence in *Pseudomonas aeruginosa* PA14. *Infect. Immun.* 73, 4399–4403. doi: 10.1128/IAI.73.7.4399-4403.2005

Leimkuhler, S., Buhning, M., and Beilschmidt, L. (2017). Shared sulfur mobilization routes for tRNA thiolation and molybdenum cofactor biosynthesis in prokaryotes and eukaryotes. *Biomolecules* 7:5. doi: 10.3390/biom7010005

Ma, J. C., Wu, Y. Q., Cao, D., Zhang, W. B., and Wang, H. H. (2017). Only Acyl carrier protein 1 (AcpP1) functions in *Pseudomonas aeruginosa* fatty acid synthesis. *Front. Microbiol.* 8:2186. doi: 10.3389/fmicb.2017.02186

Marcq, S., Diaz-Ruano, A., Charlier, P., Dideberg, O., Tricot, C., Pierard, A., et al. (1991). Molecular size and symmetry of *Pseudomonas aeruginosa* catabolic ornithine carbamoyltransferase. An X-ray crystallography analysis. *J. Mol. Biol.* 220, 9–12. doi: 10.1016/0022-2836(91)90375-G

Mishra, S., and Imlay, J. (2012). Why do bacteria use so many enzymes to scavenge hydrogen peroxide? *Arch. Biochem. Biophys.* 525, 145–160. doi: 10.1016/j.abb.2012.04.014

Ochsner, U., and Reiser, A. J. (1995). Autoinducer-mediated regulation of rhamnolipid biosurfactant synthesis in *Pseudomonas aeruginosa*. *Proc. Natl. Acad. Sci. U.S.A.* 92, 6424–6428. doi: 10.1073/pnas.92.14.6424

Ochsner, U. A., Vasil, A. I., and Vasil, M. L. (1995). Role of the ferric uptake regulator of *Pseudomonas aeruginosa* in the regulation of siderophores and exotoxin A expression: purification and activity on iron-regulated promoters. *J. Bacteriol.* 177, 7194–7201. doi: 10.1128/jb.177.24.7194-7201.1995

Ou, P., and Wolff, S. P. (1996). A discontinuous method for catalase determination at 'near physiological' concentrations of H2O2 and its application to the study of H2O2 fluxes within cells. *J. Biochem. Biophys. Methods* 31, 59–67. doi: 10.1016/0165-022X(95)00039-T

Parris, K. D., Lin, L., Tam, A., Mathew, R., Hixon, J., Stahl, M., et al. (2000). Crystal structures of substrate binding to *Bacillus subtilis* holo-(acyl carrier protein) synthase reveal a novel trimeric arrangement of molecules resulting in three active sites. *Structure* 8, 883–895. doi: 10.1016/S0969-2126(00)00178-7

Parsek, M. R., Schaefer, A. L., and Greenberg, E. P. (1997). Analysis of random and site-directed mutations in rhII, a *Pseudomonas aeruginosa* gene encoding

an acylhomoserine lactone synthase. *Mol. Microbiol.* 26, 301–310. doi: 10.1046/j.1365-2958.1997.5741935.x

Rafi, S., Novichenok, P., Kolappan, S., Stratton, C. F., Rawat, R., Kisker, C., et al. (2006). Structure of acyl carrier protein bound to FabI, the FASII enoyl reductase from *Escherichia coli*. *J. Biol. Chem.* 281, 39285–39293. doi: 10.1074/jbc.M608758200

Ramos-Vega, A. L., Davila-Martinez, Y., Sohlenkamp, C., Contreras-Martinez, S., Encarnacion, S., Geiger, O., et al. (2009). SMb20651 is another acyl carrier protein from *Sinorhizobium meliloti*. *Microbiology* 155, 257–267. doi: 10.1099/mic.0.022079-0

Rao, X., Huang, X., Zhou, Z., and Lin, X. (2013). An improvement of the 2^(-delta delta CT) method for quantitative real-time polymerase chain reaction data analysis. *Biostat. Bioinforma. Biomath.* 3, 71–85.

Raychaudhuri, A., Jerga, A., and Tipton, P. A. (2005). Chemical mechanism and substrate specificity of rhlI, an acylhomoserine lactone synthase from *Pseudomonas aeruginosa*. *Biochemistry* 44, 2974–2981. doi: 10.1021/bi048005m

Salunkhe, P., Topfer, T., Buer, J., and Tummler, B. (2005). Genome-wide transcriptional profiling of the steady-state response of *Pseudomonas aeruginosa* to hydrogen peroxide. *J. Bacteriol.* 187, 2565–2572. doi: 10.1128/JB.187.8.2565-2572.2005

Schneider, C. A., Rasband, W. S., and Eliceiri, K. W. (2012). NIH Image to ImageJ: 25 years of image analysis. *Nat. Methods* 9, 671–675. doi: 10.1038/nmeth.2089

Schuster, M., Lostroh, C. P., Ogi, T., and Greenberg, E. P. (2003). Identification, timing, and signal specificity of *Pseudomonas aeruginosa* quorum-controlled genes: a transcriptome analysis. *J. Bacteriol.* 185, 2066–2079. doi: 10.1128/jb.185.7.2066-2079.2003

Schweizer, H., and Po, P. C. (1996). Regulation of glycerol metabolism in *Pseudomonas aeruginosa*: characterization of the glpR repressor gene. *J. Bacteriol.* 178, 5215–5221. doi: 10.1128/jb.178.17.5215-5221.1996

Scoffield, J., and Silo-Suh, L. (2016). Glycerol metabolism promotes biofilm formation by *Pseudomonas aeruginosa*. *Can. J. Microbiol.* 62, 704–710. doi: 10.1139/cjm-2016-0119

Shin, D. H., Choi, Y. S., and Cho, Y. H. (2008). Unusual properties of catalase A (KatA) of *Pseudomonas aeruginosa* PA14 are associated with its biofilm peroxide resistance. *J. Bacteriol.* 190, 2663–2670. doi: 10.1128/JB.01580-07

Stirling, C. J., Colloms, S. D., Collins, J. F., Szatmari, G., and Sherratt, D. J. (1989). xerB, an *Escherichia coli* gene required for plasmid ColE1 site-specific recombination, is identical to pepA, encoding aminopeptidase A, a protein with substantial similarity to bovine lens leucine aminopeptidase. *EMBO J.* 8, 1623–1627.

Therisod, H., and Kennedy, E. P. (1987). The function of acyl carrier protein in the synthesis of membrane-derived oligosaccharides does not require its phosphopantetheine prosthetic group. *Proc. Natl. Acad. Sci. U.S.A.* 84, 8235–8238. doi: 10.1073/pnas.84.23.8235

Therisod, H., Weissborn, A. C., and Kennedy, E. P. (1986). An essential function for acyl carrier protein in the biosynthesis of membrane-derived oligosaccharides of *Escherichia coli*. *Proc. Natl. Acad. Sci. U.S.A.* 83, 7236–7240. doi: 10.1073/pnas.83.19.7236

Tricot, C., Nguyen, V. T., and Stalon, V. (1993). Steady-state kinetics and analysis of pH dependence on wild-type and a modified allosteric *Pseudomonas aeruginosa* ornithine carbamoyltransferase containing the replacement of glutamate 105 by alanine. *Eur. J. Biochem.* 215, 833–839. doi: 10.1111/j.1432-1033.1993.tb18099.x

Tricot, C., Villeret, V., Sainz, G., Dideberg, O., and Stalon, V. (1998). Allosteric regulation in *Pseudomonas aeruginosa* catabolic ornithine carbamoyltransferase revisited: association of concerted homotropic cooperative interactions and local heterotropic effects. *J. Mol. Biol.* 283, 695–704. doi: 10.1006/jmbi.1998.2133

Turner, K. H., Everett, J., Trivedi, U., Rumbaugh, K. P., and Whiteley, M. (2014). Requirements for *Pseudomonas aeruginosa* acute burn and chronic surgical wound infection. *PLoS Genet.* 10:e1004518. doi: 10.1371/journal.pgen.1004518

Van Vranken, J. G., Jeong, M. Y., Wei, P., Chen, Y. C., Gygi, S. P., Winge, D. R., et al. (2016). The mitochondrial acyl carrier protein (ACP) coordinates mitochondrial fatty acid synthesis with iron sulfur cluster biogenesis. *eLife* 5:e17828. doi: 10.7554/eLife.17828

Venturi, V. (2006). Regulation of quorum sensing in *Pseudomonas*. *FEMS Microbiol. Rev.* 30, 274–291. doi: 10.1111/j.1574-6976.2005.00012.x

Viala, J. P., Prima, V., Puppo, R., Agrebi, R., Canestrari, M. J., Lignon, S., et al. (2017). Acylation of the Type 3 secretion system translocon using a dedicated Acyl carrier protein. *PLoS Genet.* 13:e1006556. doi: 10.1371/journal.pgen.1006556

Volkmann, G., Murphy, P. W., Rowland, E. E., Cronan, J. E. Jr., Liu, X. Q., Blouin, C., et al. (2010). Intein-mediated cyclization of bacterial acyl carrier protein stabilizes its folded conformation but does not abolish function. *J. Biol. Chem.* 285, 8605–8614. doi: 10.1074/jbc.M109.060863

Wagner, V. E., Bushnell, D., Passador, L., Brooks, A. I., and Iglewski, B. H. (2003). Microarray analysis of *Pseudomonas aeruginosa* quorum-sensing regulons: effects of growth phase and environment. *J. Bacteriol.* 185, 2080–2095. doi: 10.1128/jb.185.7.2080-2095.2003

Winsor, G. L., Griffiths, E. J., Lo, R., Dhillon, B. K., Shay, J. A., and Brinkman, F. S. (2016). Enhanced annotations and features for comparing thousands of *Pseudomonas* genomes in the *Pseudomonas* genome database. *Nucleic Acids Res.* 44, D646–D653. doi: 10.1093/nar/gkv1227

Woolwine, S. C., and Wozniak, D. J. (1999). Identification of an *Escherichia coli* pepA homolog and its involvement in suppression of the algB phenotype in mucoid *Pseudomonas aeruginosa*. *J. Bacteriol.* 181, 107–116.

Zhang, Y.-M., Frank, M. W., Zhu, K., Mayasundari, A., and Rock, C. O. (2008). PqsD is responsible for the synthesis of 2,4-dihydroxyquinoline, an extracellular metabolite produced by *Pseudomonas aeruginosa*. *J. Biol. Chem.* 283, 28788–28794. doi: 10.1074/jbc.M804555200

Zhang, Y. M., Marrakchi, H., and Rock, C. O. (2002). The FabR (YijC) transcription factor regulates unsaturated fatty acid biosynthesis in *Escherichia coli*. *J. Biol. Chem.* 277, 15558–15565. doi: 10.1074/jbc.M201399200

Zhang, Y.-M., and Rock, C. O. (2012). Will the initiator of fatty acid synthesis in *Pseudomonas aeruginosa* please stand up? *J. Bacteriol.* 194, 5159–5161. doi: 10.1128/jb.01198-12

Zhou, J.-Y., Afjehi-Sadat, L., Asress, S., Duong, D. M., Cudkowicz, M., Glass, J. D., et al. (2010). Galectin-3 is a candidate biomarker for amyotrophic lateral sclerosis: discovery by a proteomics approach. *J. Proteome Res.* 9, 5133–5141. doi: 10.1021/pr100409r